

Preparation and yielding behavior of pendular network suspensions

Junyi Yang, and Sachin S. Velankar

Citation: *Journal of Rheology* **61**, 217 (2017);

View online: <https://doi.org/10.1122/1.4973962>

View Table of Contents: <http://sor.scitation.org/toc/jor/61/2>

Published by the [The Society of Rheology](#)

Articles you may be interested in

[Rheology of fumed silica/polydimethylsiloxane suspensions](#)

Journal of Rheology **61**, 205 (2017); 10.1122/1.4973974

[Oscillations and damping in the fractional Maxwell materials](#)

Journal of Rheology **61**, 187 (2017); 10.1122/1.4973957

[The performance of the hot end in a plasticating 3D printer](#)

Journal of Rheology **61**, 229 (2017); 10.1122/1.4973852

[Molecular mechanisms of interfacial slip for polymer melts under shear flow](#)

Journal of Rheology **61**, 253 (2017); 10.1122/1.4974907

[Relaxation time of dilute polymer solutions: A microfluidic approach](#)

Journal of Rheology **61**, 327 (2017); 10.1122/1.4975933

[Microstructure, phase inversion and yielding in immiscible polymer blends with selectively wetting silica particles](#)

Journal of Rheology **61**, 363 (2017); 10.1122/1.4975931



**Your future-proof
rheometer.**

MCR 702 TwinDrive™

Get in touch: www.anton-paar.com



Preparation and yielding behavior of pendular network suspensions

Junyi Yang

Department of Chemical and Petroleum Engineering, University of Pittsburgh, Pittsburgh, Pennsylvania 15260

Sachin S. Velankar^{a)}

Department of Chemical and Petroleum Engineering, University of Pittsburgh, Pittsburgh, Pennsylvania 15260 and Department of Mechanical Engineering and Materials Science, University of Pittsburgh, Pittsburgh, Pennsylvania 15260

(Received 6 August 2016; final revision received 10 November 2016; published 20 January 2017)

Abstract

Particles suspended in a less-wetting fluid can be aggregated by addition of a small quantity of an immiscible fluid that preferentially wets the particles. If the added wetting fluid is sufficiently dilute, the aggregates are composed of particles held together by pendular menisci of the wetting fluid. Such pendular aggregates can then percolate into a network which endows the suspension with a yield stress. We examine the yielding behavior of pendular networks at a particle volume fraction of 20%, with wetting fluid loadings ranging from 0.08% to 6.4%. Steady shear experiments give a dynamic yield stress that increases roughly linearly with wetting fluid loading within the pendular regime, and the shear stress vs shear rate behavior can be collapsed onto a mastercurve by simply normalizing the stress by the yield stress. Linear viscoelastic moduli are found to decrease if the suspensions are sheared at a high rate prior to the modulus measurement, but this decrease can be reversed by shearing at a low rate. Various measures of yielding—the limit of linear viscoelastic behavior, the crossover of the storage and loss moduli in large amplitude oscillatory shear experiments, and strain recoil after cessation of shear—all suggest that the networks yield at $\sim 1\%$ strain. This strain is much smaller than expected from the micromechanics of rupturing pendular menisci, and we suggest nonhomogeneous deformation of the networks as the reason for the discrepancy. © 2017 Author(s). All article content, except where otherwise noted, is licensed under a Creative Commons Attribution (CC BY) license (<http://creativecommons.org/licenses/by/4.0/>). [<http://dx.doi.org/10.1122/1.4973962>]

I. INTRODUCTION

In particulate systems, capillary forces can bind discrete particles together into a space-spanning network with a yield stress. The most familiar example is of sand which, when wetted with small amounts of water, develops sufficient yield stress to allow construction of elaborate sand castles [1–4]. The same is true for particles-in-liquid suspensions: Addition of a small amount of a second immiscible liquid can create a network which endows the suspension with a yield stress [5–14].

Such suspensions in which capillarity forces are important are practically useful in materials science. Specifically, the very simple method—“add liquid and mix”—of realizing a yield stress offers a convenient way of stabilizing a structure temporarily before it can be made permanent, e.g., by sintering or crosslinking [15]. Furthermore, open pore morphologies can be realized readily in such systems [9,16–18] with immediate relevance to applications in which chemical transport or fluid retention must be combined with mechanical strength. Indeed applications to materials science are not restricted to suspensions with capillary forces—a diverse set of particle/fluid/liquid

mixtures can, depending on the materials and composition, yield a variety morphologies of potential interest to materials science [15], including Pickering emulsions [8,19], particle-stabilized foams [20–22], bijels [18,23], wet granular materials [1,24,25], and liquid marbles [26,27].

In such particulate systems with capillarity, the wettability of the particles toward the minority liquid plays a crucial role in determining the suspension microstructure [15,28,29]. The above-mentioned case of wet sand is, in this article, dubbed the *fully wetting* situation, i.e., the particles are fully wetted by the minority liquid, water. The case when the particles are less-favorably wetted by the minority fluid is dubbed the *partially wetting* situation. This article is concerned with the former situation.

In a previous paper [12], we examined the morphology of suspensions in the fully wetting situation. The suspensions were composed of two immiscible polymeric liquids and silica particles that were fully wetted by one of the two liquids. Experiments showed that when the wetting liquid was present in a small minority (in that paper, 16 vol. % of the particle loading), the morphology consisted of particles bound together by small menisci of the wetting liquid. At very low particle loadings, such meniscus binding led to the formation of open (i.e., not compact) aggregates denoted *pendular aggregates*. When the particle loading exceeded a few percent, aggregates were found to join together into a percolating network which was dubbed a *pendular network*. This

^{a)}Author to whom correspondence should be addressed; electronic mail: velankar@pitt.edu

terminology derives from the term *pendular meniscus* used to describe an hourglass-shaped meniscus joining two particles [25,30,31], which is our idealized picture of the basic building block of a network at low wetting fluid loadings. Rheologically, pendular networks were found to behave analogous to other attractive suspensions: They show yield stress in steady shear, solidlike behavior, G' - G'' crossover in large amplitude oscillatory shear (LAOS), and delayed yielding in creep [12].

The goal of this article is to examine the rheology of pendular networks in greater detail, for example, quantifying how the yield strain changes with the wetting liquid loading, whether the networks have significant elasticity (in the sense of elastic recoil), and whether rheological properties can be related to microstructural details of the pendular bridges. A significant part of this paper is devoted to the effect of shear history on the rheological properties. Specifically as will be discussed in Sec. IV, pendular menisci are associated with a certain attractive force, and furthermore, the meniscus breaks when the interparticle distance is sufficiently large. This raises an obvious question: Can a high preshear rate or a high preshear strain disrupt the pendular network and induce softening? On the other hand, a meniscus may also be re-formed under applied flow as particles that already have wetting fluid on their surface come into contact with each other. This raises a second question: Can changes in rheological properties be restored by sufficiently long flow? Or is flow-induced structural breakdown long-lived, and thus induce nearly permanent changes in properties? Furthermore, since a pendular meniscus can be stretched to some extent without rupture, can this induce viscoelastic phenomena in the suspension such as elastic recovery after cessation of shear?

Incidentally, very similar questions have been addressed in another system with capillary forces, viz., droplet-matrix blends of immiscible fluids. In that case, flow induces both drop breakup and drop coalescence (analogous to breaking and reforming menisci). In those systems, shearing at high rate can reduce drop size and affect the rheology, but subsequent shearing at lower rate can usually (but not always) restore the original drop size and rheological properties [32–34]. Furthermore, the increase in interfacial area due to applied flow provides a means of storing mechanical energy and hence induces viscoelastic effects [35–37]. This article seeks to address similar questions for particulate systems with capillary forces.

This paper is structured as follows: Section II provides experimental details, and Sec. III discusses the experiments. In the first part of Sec. III, we develop and validate a new method for preparing our three-component mixtures along with a rationale for why this new method is preferred over the mixing procedures followed previously. In Sec. III B, we address the questions of the previous paragraph through rheological experiments. Section IV comments on the results in the context of the micromechanics of meniscus rupture, followed by Conclusions.

II. EXPERIMENTAL

A. Materials

Polyisobutylene (PIB, $\rho \approx 0.908$ g/ml, $M_w \approx 2200$ g/mol) and polyethylene oxide (PEO, $\rho \approx 1.1$ g/ml, $M_w \approx 20\,000$ g/mol, melting point $\approx 65^\circ\text{C}$) were purchased from Soltex and Fluka, respectively. Spherical silica particles (diameter roughly $2\ \mu\text{m}$) were purchased from Industrial Powders. All experimental materials are identical to those used previously [10,12,14]. As shown previously [10,12], the particle surfaces are fully wetted by PEO, which is the minority phase in the mixtures examined here.

B. Sample preparation

A small quantity of PIB and PEO were mixed together to make a concentrated “masterbatch” using a custom ball mixer [38]. PIB (80 wt.%) and PEO (20 wt.%) were held inside the mixer at 80°C for 15 min to ensure complete melting, and then mixed at 500 rpm for 5 min. The mixed product was then transferred into a sealed plastic dish, kept in the refrigerator at about 10°C for at least 30 min to complete crystallization of the PEO. The masterbatch blend has a PEO-in-PIB morphology, and after dissolving the PIB, the residual PEO drops are seen to be roughly $5\ \mu\text{m}$ in diameter (Fig. 1).

Ternary samples of the desired composition were prepared by blending appropriate quantities of this masterbatch, pure PIB, and particles. This blending was performed by hand with a spatula in a 40 mm petri dish at room temperature. Samples were placed in vacuum overnight to degas. This mixing procedure is different than that used previously [12], and the reasons for this will be discussed in Sec. III.

C. Rheology and characterization

Rheological experiments were conducted on a TA Instruments AR-2000 stress-controlled rheometer as well as Anton Paar rheometer MCR 302. All the experiments were carried out on a 25 mm parallel plate geometry profiled to prevent wall slip, at 80°C to ensure that PEO was well above its melting temperature. The geometry was preheated to 80°C the sample loaded, and set to a gap of no more than 1 mm.

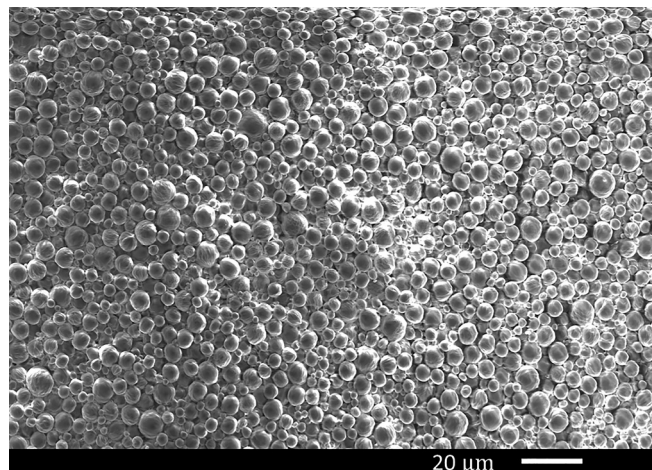


FIG. 1. SEM image of solidified PEO dispersed phase drops extracted from the masterbatch. (enhanced online) [URL: <http://dx.doi.org/10.1122/1.4973962.1>]

Both continuous and oscillatory shear flow properties were measured. For continuous shear, steady shear measurements were conducted at shear rates increasing from 0.01 to 100 s^{-1} . Each shear rate was maintained for 1 min. Creep-recovery tests were done at stresses lower than the yield stress estimated from steady shear measurements. Creep times were varied (discussed later), whereas a fixed recovery time of 250 s was set. For oscillatory experiments, amplitude sweep tests (strain ranging from 0.005% up to 300% at 1 rad/s) were conducted.

The compositions selected here are firmly in the regime in which pendular aggregates are expected, and hence, morphological characterization is not the focus here. A limited amount of optical and electron microscopy was conducted using methods established previously. These show that the samples have the expected structure of pendular aggregates, viz., particles which are connected by small menisci of the PEO. A typical example of the morphology is shown in Fig. S1 in the supplementary material [39].

III. RESULTS

A. Validation of the “cold mixing”

Our previous research [10] considered ternary mixtures using the same constituents as the present paper with a composition of 10 vol. % particles and 2.8 vol. % PEO. Various mixing methods were considered, including premixing the particles into the PIB before adding the PEO or vice versa (predisperse the PEO before adding particles). Different combinations of mixing speed were also used. In all cases, the temperature during the mixing was 80°C , and hence, the PEO was molten when it was mixed. In general, two types of structures were evident: A network of particles bound by menisci of PEO, and large PEO-bound particle aggregates, called *capillary aggregates*. For convenience, examples of both structures, taken from that article [10], are shown in supplementary Fig. S1 [39]. That article suggested that capillary aggregates were a “trapped state” which could not be broken up easily under mixing conditions. Achieving predominantly pendular networks required avoiding the formation of capillary aggregates in the first place, e.g., by predispersing the wetting fluid PEO (preferably at a size smaller than of the particles) prior to adding particles.

Despite success in avoiding capillary aggregates, the previous methods still have some limitations. The first is that research on wet granular materials suggests that even extremely small quantities of wetting fluid (as low as 0.01 vol. %) can affect the flow behavior [2]. Previously [12], we conducted experiments with wetting fluids volume fractions as low as $\phi_{\text{PEO}} = 0.16\%$ and found that pendular aggregation already had a major effect on rheological properties. For a $\sim 4\text{-g}$ batch, this volume fraction corresponds to only 8 mg of wetting fluid. Apart from possible errors in weighing such small quantities, it is also possible that some of the wetting fluid may be “lost” if it wets the internal parts of the mixer, making the actual mixture composition different from the target value. Accordingly, volume fractions of wetting fluid lower than 0.16% were not examined. Second, the previous experiments showed that the size of the drops immediately prior to adding particles is an

important parameter affecting the morphology development, with a small drop size reducing the formation of capillary aggregates. But when the PEO/PIB ratio is itself varied, the drop size may change, and this may be expected to affect the morphology. Finally, reproducing the same morphology using a different mixer, e.g., one with a larger capacity, is difficult, once again because different mixing characteristics are likely to create different drop sizes prior to adding particles.

The mixing process considered here, dubbed cold mixing is intended to circumvent these problems. Analogous to one of our previous mixing processes, the PEO is predispersed as drops in the PIB, but then, the blend masterbatch is cooled to solidify the PEO drops (shown in Fig. 1). Particles are then mixed with this masterbatch at room temperature (along with additional PIB as needed). The sample is then heated in a rheometer to remelt the PEO drops, and then sheared to induce meniscus-bridging of particles. This cold mixing method offers several advantages. First, since samples in the pendular regime require very little PEO, a single PEO/PIB masterbatch is adequate to prepare a large number of ternary samples. Since the size of the frozen drops does not change during the room-temperature mixing step, all the ternary samples have identical drop size distributions across all samples. Second, the masterbatch can be diluted repeatedly to realize very low wetting fluid loadings without significant weighing errors, and moreover, since the PEO is solid until the sample is loaded in the rheometer, it cannot be lost by wetting parts of the mixer (the mixing dish and spatula in our case). Finally, any method may be used to prepare the masterbatch, including any convenient batch mixer (our method), extrusion, or even precipitation from a common solvent. The first task of this paper therefore is to validate this cold mixing method as a means of preparing pendular morphologies.

Figure 2 validates this cold mixing approach. It compares the oscillatory behavior in amplitude sweep experiments for one specific blend with 20 vol. % particles and 3.2 vol. % PEO before melting vs after melting and shearing. The oscillatory behavior of the cold-mixed sample at 30°C (“-” symbols with thick curves) suggests liquidlike behavior with $G'' \gg G'$ over the entire strain range. Such behavior is consistent with that expected for a suspension with a dispersed phase loading of 23.2 vol. %. Note that the silica particles as well as the solidified PEO drops are both more polar than the PIB matrix, and this suspension is expected to behave not like a hard-sphere suspension but like a suspension of attractive particles. Indeed supplementary Fig. S2 [39] shows that under steady shear conditions at 30°C , this blend is somewhat shear-thinning, likely reflecting the influence of attractive interactions.

The sample was then melted, and sheared at 1 s^{-1} for 10 min. Upon repeating the amplitude sweep, a sharp change in rheology is apparent in Fig. 2: $G'' < G'$ at low strain, followed by a crossover at intermediate strain. Such behavior is qualitatively similar to that observed in our previous research at the same composition and was attributed to the formation of a pendular network (i.e., with pendular menisci bridging the particles), and the strain crossover was interpreted in terms of the microstructural breakdown of these menisci. This will be discussed further later. Subsequent to the amplitude sweep, the steady shear viscosity was measured at

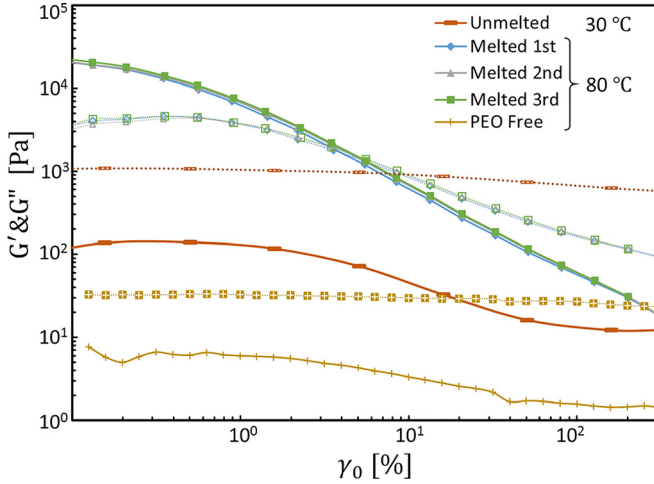


FIG. 2. LAOS results for ternary mixture (PIB/PEO/silica = 76.8/3.2/20) before and after melting, and binary suspension (PIB/silica = 76.8/23.2). Filled symbols with solid lines represent the storage modulus and open symbols with dashed lines represent the loss modulus.

several different rates, and once again, the behavior (Fig. S2 [39]) is qualitatively different from the unmelted sample: The sample shows yield-stress rheology (viscosity roughly follows $\dot{\gamma}^{-1}$) similar to that obtained from pendular networks previously [12].

Figures 2 and S2 [39] also show the behavior of a particles-in-PIB mixture without any PEO added at 80 °C, and this suspension is liquidlike, not surprising for a suspension at 20 vol. % particles. Thus, as previously, we firmly conclude that the strongly non-Newtonian behavior is attributable to capillary forces between particles.

In Sec. III C we will show that deformation history affects LAOS behavior significantly. Anticipating that, it is immediately relevant to ask whether the measured rheology changed if the sample was sheared for a longer duration. Accordingly, Fig. 2 shows two additional LAOS experiments, each conducted with an additional 600 strain units of shear at the same shear rate of 1 s^{-1} . These show negligible differences in moduli as compared to the first shearing step, suggesting that sufficiently long shearing can establish a steady state rheology, at least under the conditions of Fig. 2.

B. Rheological changes with wetting fluid content

The cold-mixing approach can now be applied to examine the effect of wetting fluid content on the rheology. Previously, we had shown that the rheological properties are nonmonotonic in wetting fluid loading: At very low wetting fluid loadings, the formation of a pendular network led to the rheological changes detailed in Figs. 2 and S2 [39]. But once the wetting fluid volume fraction became comparable to the particle fraction, the wetting fluid encapsulated the particles leading to a destruction of the pendular morphology, and the solidlike rheology diminished. The corresponding results are best-represented in terms of the wetting fluid to particle volume ratio: $\varrho = \phi_{\text{PEO}}/\phi_p$: Samples with ϱ of about 0.1–0.3 had a roughly pendular structure, whereas in samples with ϱ exceeding 1, the particles were engulfed by the wetting fluid, and had a diminished yield stress.

We seek to repeat those experiments for two reasons. First, as mentioned in the Introduction, preparing samples by direct mixing of the three components sometimes involved very small quantities of wetting fluid, with consequent uncertainty in composition. Second, more important, even the lowest wetting fluid loading that could be examined previously already showed a measurable yield stress. Thus, we were not able to capture the transition between liquid and solid as fluid loading is increased. For instance, we could not establish whether there is a minimum amount of wetting fluid needed for developing a yield stress, or equivalently, if the yield stress appears gradually or abruptly as wetting fluid content changes. As mentioned above, one advantage of the cold mixing approach is that since mixing is performed when the PEO droplets are frozen, low wetting fluid loadings can be realized by sequential dilution. Accordingly, we examined the rheology of 20 vol. % silica suspensions with PEO loadings varying from $\phi_{\text{PEO}} = 0.08\%$ to 6.4%. These results are shown in Fig. 3. The numbers in the legend correspond to the value of ϱ , but since the particle loading is fixed at 20 vol. %, the ϕ_{PEO} values are simply $0.2 \times \varrho$.

In the absence of PEO, the particles-in-PIB suspension show strain sweep behavior similar to that of the unmelted sample in Fig. 2: Liquidlike rheology with $G'' \gg G'$ over the entire strain range. Addition of wetting fluid at a loading $\phi_{\text{PEO}} = 0.08\%$ (which corresponds to $\varrho = 0.004$) has only a slight effect on the moduli. The next higher wetting fluid loading, corresponding to $\varrho = 0.016$ already shows all the features of the pendular network that were evident in Fig. 2: Much higher moduli, $G' > G''$ at low frequencies, and then a moduli crossover at some strain. Further increase in wetting fluid loading does not change the behavior qualitatively but quantitatively, the moduli increase considerably up to $\varrho = 0.25$, followed by a modest decrease.

In steady shear [Fig. 3(b)], the effects of PEO are felt even at the lowest PEO loading where the low-rate viscosity rises significantly at $\varrho = 0.004$. Upon further addition of PEO, the low-rate data show a clear yield stress, whereas there is only a modest change in stress at the highest shear rates accessible, and the stress vs strain rate data approach a slope of 1. These results suggest that significant solidlike behavior appears between $\phi_{\text{PEO}} = 0.08\%$ and 0.32% corresponding to $\varrho = 0.004$ and 0.016. It is difficult to reliably measure the value of yield stress at very low wetting fluid loadings. Hence, it is difficult to establish a percolation threshold above which a space-spanning network exists. Indeed, there does not appear to be any wetting fluid loading at which the yield stress increases abruptly.

To quantify the yield stress in a consistent fashion across all samples, the data of Fig. 3(b) were fitted to the modified Herschel Bulkley equation

$$\sigma = \sigma_y + k * \dot{\gamma}^n + \eta_\infty * \dot{\gamma}, \quad (1)$$

where σ_y represent the yield stress, the first two terms on the right hand side compose the “standard” Herschel and Bulkley expression [40], and the last term is a Newtonian term which guarantees that the viscosity approaches a finite value of η_∞ at high rates. Note that the $\eta_\infty * \dot{\gamma}$ term on the

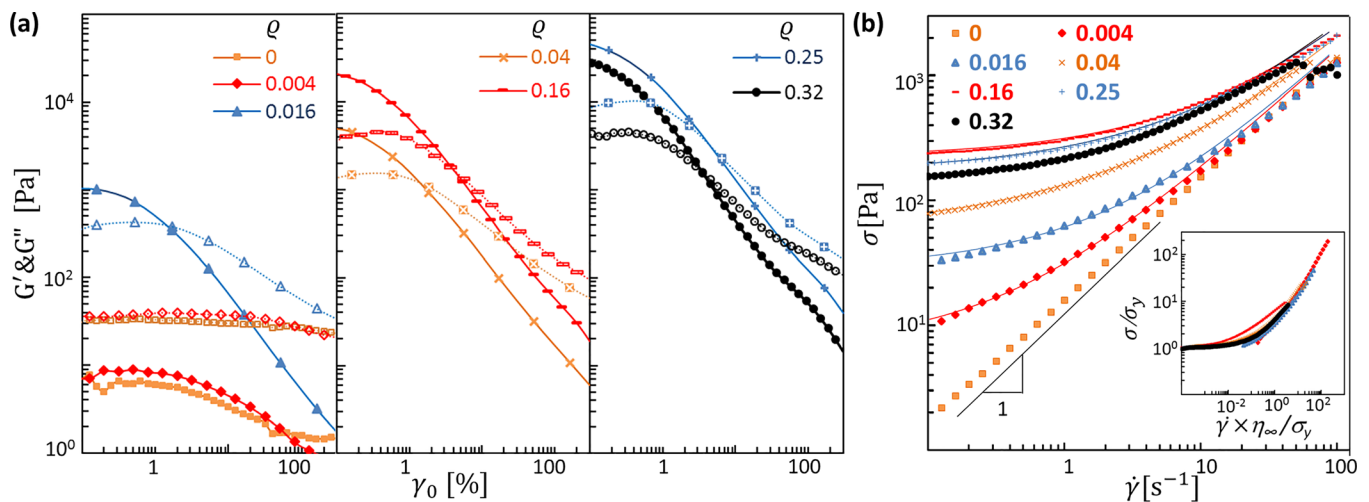


FIG. 3. (a) LAOS results for ternary mixtures at fixed particle loading (20 vol. %) and various ρ values listed in the legend. Filled symbols with solid lines represent the storage modulus and open symbols with dashed lines represent the loss modulus; (b) Steady state stress under various shear rates for the same ternary blends. Solid lines represent the best fit for each composition using Eq. (1). The inset shows normalized plots for the same data.

right hand side was missing in Domenech and Velankar [12]. The value of η_∞ is set to the measured viscosity of the particles-in-PIB suspensions (without PEO added) and hence is not a fitting parameter; this is discussed further below. The data of Fig. 3(b) were fitted to Eq. (1) with σ_y , k , and n as fitting parameters. The solid lines in Fig. 3(b) show the fits, and the corresponding values of the three fitting parameters are given in Table I. The value of n is found to be close to 0.5 for all the samples. The fitted yield stress [Fig. 4(a)] increases almost linearly at low ϕ_{PEO} values, followed by a decrease in yield stress when ρ exceeds 0.16 (i.e., ϕ_{PEO} exceeds 3.2%). As a caveat, it must be noted that the yield stress obtained at the lowest ρ value may not be entirely accurate since those stress vs rate data do not show a clear plateau at low rates. Furthermore, the lowest 2–3 points in Fig. 3(b) may not have reached steady shear conditions due to the low shear strain corresponding to the 1 min shearing time. It is useful to compare the results against those obtained previously [12]. The first comparison is against the yield stress measured at same composition, but prepared by the previous mixing method in which the PEO drops were molten during mixing. That case gave a somewhat higher yield stress (green triangle). The second is a series of ternary mixtures at 10 vol. % particles, but spanning roughly the same range of ρ values. The corresponding yield stresses [shown by the red squares in Fig. 4(a)] are qualitatively similar, and in particular, at both 10 and 20 vol. % particles,

TABLE I. Summary of fitting parameters used in modified Herschel–Bulkley equation: $\sigma = \sigma_y + k * \dot{\gamma}^n + \eta_\infty * \dot{\gamma}$ for various ρ values. Fits are shown as solid lines in Fig. 3(b).

$\rho = \frac{\phi_{PEO}}{\phi_p}$	k (SI units)	n	σ_y (Pa)
0.004	11.1	0.552	6.70
0.016	20.2	0.448	27.3
0.04	64.2	0.443	55.1
0.16	78.5	0.485	220.7
0.25	85.7	0.478	169.0
0.32	72.6	0.552	134.3

samples approximately show the $\sigma_y \propto \phi_{PEO} \propto \rho$ at low wetting fluid loadings and then a maximum yield stress when ρ is on the order of 0.1.

Finally, we previously suggested a two-parameter scaling of the flow curve. Specifically, we proposed scaling the steady shear data as follows: (1) normalize the shear stress by the yield stress σ_y , (2) the viscosity by the limiting high shear rate, viscosity η_∞ , and (3) as a consequence, normalize the shear rate by the characteristic rate σ_y/η_∞ . This scaling is suggested by drawing an analogy between suspensions in a pendular state and suspensions with attractive interactions between particles [12,41]. At sufficiently low shear rates, viscous forces are negligible, and hence, the stress (which approaches the yield stress) embodies the attractive forces between particles. At sufficiently high rates viscous forces dominate, and hence, the stress must simply represent the hard-sphere type contribution of the particles. In this physical picture, just two parameters—the yield stress that represents interparticle attractions, and the high-shear rate viscosity that represents viscous interactions between particles—suffice to scale all the steady shear behavior. Here, we test whether the scaling applies as the PEO loading (rather than the particle loading) is varied. Since all the samples of Fig. 3 have the same particle loading (20 vol. %), they must necessarily have the same value of η_∞ , and indeed, we remarked above that the high-shear rate stress is only weakly sensitive to wetting fluid loading. Thus, $\eta_\infty = 12.6$ Pa s (the viscosity of the PEO-free blend at 20 vol. % particle loading) is assigned to all the samples [this is also why η_∞ was not a fitting parameter when Eq. (1) was used above]. The only “shift” permissible is to normalize the stress using the yield stress. Figure 4(b) shows the results. With no further adjustable parameters [since σ_y was already determined in Fig. 4(a)], a reasonable superposition of the various flow curves is obtained. The same scaling is shown in the form of a normalized stress vs normalized rate graph as an inset in Fig. 3(b). This confirms the validity of treating the flow curve of pendular suspensions as being an “interpolation” between a low rate regime dominated by

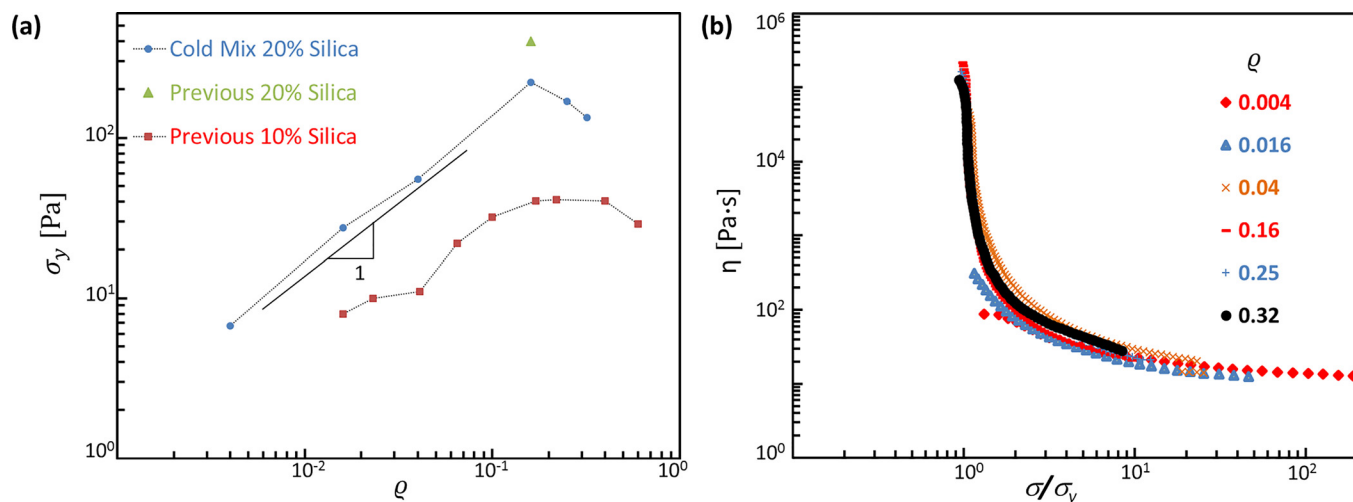


FIG. 4. (a) Yield stresses at various ϕ values corresponding to Fig. 3(b) and compared with previous results. (b) Viscosity versus normalized shear rate curves for ternary mixture with 20 vol. % silica at various ϕ values.

capillary attractions, and a high rate regime dominated by hard sphere suspension hydrodynamics. We must reiterate that at $\phi = 0.004$, the flow curve is only weakly non-Newtonian [Fig. 3(b)], and therefore, the corresponding value of yield stress is susceptible to some error.

C. Dependence of flow conditions on microstructure and its effects on yielding

As explained in the Introduction, since such ternary blends are far from equilibrium, their microstructure can depend significantly on their deformation history. We have already mentioned that adding the PEO after the particles led to the formation of numerous capillary aggregates, whereas predispersing the PEO before adding the particles gave a pendular structure with an almost complete absence of capillary aggregates. That same article [10] reported that different mixing approaches gave as much as a threefold difference in yield stress. At least some of the difference was attributable to the formation of capillary aggregates which, being very compact, do not contribute much to the modulus. Some of the difference might also reflect more subtle differences in microstructure such as the number of pendular bridges per unit volume or average number of bridges per particle. Regardless, since the microstructure depends on mixing conditions, it is not surprising that the rheology does too. The cold mixing approach now provides a more consistent method of preparing samples across a range of compositions, and thus permits the effect of deformation history on rheology to be examined. We are chiefly concerned with three questions, all of which arise from the physical picture of particles held together by pendular menisci. The first concerns strain rate effects: We anticipate that capillary menisci are ruptured at high stress (indeed this is equivalent to regarding η_∞ as being independent of capillary attractions between particles as discussed in Sec. III B). Does this rupture also lead to softening, i.e., to a decrease in modulus? Indeed, Koos and Willenbacher [42] measured the linear viscoelastic moduli after a high rate shearing and noted a gradual increase with time, suggesting some structural breakdown due to high rate shear, and subsequent recovery. The second

concerns strain effects: We anticipate that capillary menisci rupture when deformed sufficiently. Does such large strain-induced meniscus rupture leads to softening as well? The third concerns elasticity (in the sense of recoverable deformation): Since individual capillary menisci can be stretched (few ten percent as discussed in Sec. IV), can pendular networks show few ten percent recoverable strain after cessation of shear?

We will first illustrate the changes in rheology with deformation history with a simple shear protocol. A sample of the same composition of Fig. 2 (PIB/PEO/silica = 76.8/3.2/20) was subjected to 1 s^{-1} shear for 600 strain units, followed by an amplitude sweep at 1 rad/s up to a strain of 300%. Immediately following this, a second amplitude sweep was conducted, but with decreasing strain. A sharp decrease in low-amplitude modulus is evident [Fig. 5(a)], presumably indicating some breakdown in the structure of the particulate network. This simple experiment shows clearly that shear history can—even within a single sample—induce moduli changes of as much as a factor of five. Yet this figure does not unambiguously identify whether the softening is a rate effect or a strain effect. In an oscillatory experiment at a strain amplitude γ_0 and frequency ω , the peak strain rate is $\gamma_0\omega$. Thus, an amplitude sweep at a fixed frequency exposes samples to increasing strains as well as increasing rates.

To test the rate dependence more directly, we examined the LAOS behavior of the same composition of Fig. 2 (PIB/PEO/silica = 76.8/3.2/20) after shearing at three different rates, 0.1, 1, and 10 s^{-1} . These rates bracket the highest rate in the oscillatory experiment (3 s^{-1} corresponding to 300% strain at 1 rad/s). Each shear step was conducted for 10 min, followed by an amplitude sweep at 1 rad/s . The results [Fig. 5(b)] unambiguously show a significant softening: The low strain modulus decreases by almost three-fold after shearing the sample at 10 s^{-1} . These changes in rheology were found to be completely reversible: Upon shearing at 1 s^{-1} for 10 min, the LAOS data overlaid almost exactly onto the 1 s^{-1} results shown in Fig. 5(b). To our knowledge, these are the first data to show that the mechanical properties of suspensions with capillary interactions can be tuned reversibly by

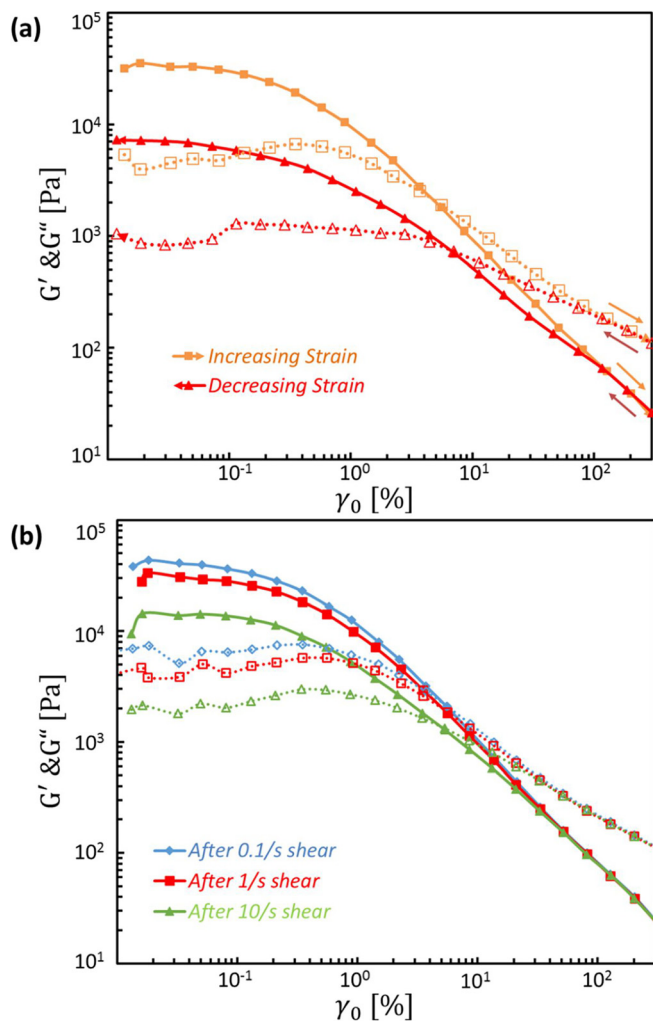


FIG. 5. (a) LAOS results for one ternary mixture (PIB/PEO/silica = 76.8/3.2/20) following a sequence of increasing strain (yellow squares) and then decreasing strain (red triangles). (b) LAOS results with increasing strain for ternary mixture at same composition after shearing at different rates. Filled symbols with solid lines represent the storage modulus and open symbols with dashed lines represent the loss modulus.

simply varying the shear rate imposed on the suspension. These experiments were performed for samples with various PEO fractions (all at 20 vol. % particles), and in all cases, LAOS data were collected after three different preshear rates. The dependence of the corresponding linear viscoelastic modulus on ϱ after the three different rates is shown in supplementary Fig. S3 [39]. All samples behave similarly (modulus reduces as preshear rate increases), but the decrease in modulus is more pronounced at low ϱ values. We speculate that this is because the capillary network becomes increasingly tenuous at low ϱ values, and can be destroyed readily by shearing. Incidentally, it is interesting to note that the trend of Fig. S3 [39]—that the modulus becomes more dependent on rate at low ϱ —cannot continue to arbitrarily low wetting fluid loadings. This is because at $\varrho = 0$, capillary interactions must vanish and the rate dependence should disappear (as indeed it does experimentally, not shown).

It is also plausible that the capillary network may be broken by strain rather than by strain rate. Specifically, the process of breaking vs remaking a pendular meniscus is

hysteretic (see Sec. IV), and hence, we examined whether a modest strain imposed on a network that was created under steady shear conditions is itself disruptive. To test the strain dependence independently of rate effects, the following shear protocol (illustrated in the upper part of Fig. 6) was used. A sample with $\phi_p = 20\%$ and $\varrho = 0.16$ was sheared at 1 s^{-1} for 600 strain units. Shearing was paused, and then resumed at the same shear rate for 1 strain unit, and then the oscillatory moduli measured. The entire process was repeated but with the latter strain being increased to 3, 60, and finally another 600 strain units. The corresponding data are shown in Fig. 6, and it is clear that while strains of about 1 strain unit do indeed reduce the modulus as compared to much longer strains *at the same rate*, these modulus variations are modest, and much smaller than those in Fig. 5. These observations suggest that while some menisci may be broken at large shear strain, new menisci are simultaneously formed, leading to little or no change in the overall network structure.

It is of immediate interest to ask whether such changes in modulus noted in Fig. 5 can be related to underlying changes in microstructure. Previously, we have used scanning electron microscopy (SEM) of samples in which the continuous phase was dissolved to qualitatively identify the microstructure (e.g., pendular vs capillary aggregates). However, that approach is not suitable for testing for more subtle changes in network microstructure since the aggregates tend to undergo at least some damage when preparing samples for SEM. Here, we attempted a different approach. Small samples of blends with 20 vol. % particles were extracted from the rheometer (from near the edge of the parallel plate geometry) after shearing at 0.1 and 10 s^{-1} shearing, and placed in a polystyrene dish. These samples were too concentrated to permit any judgment on whether structural breakdown occurred. A large drop of PIB was then placed on each sample in an attempt to gently spread out the aggregates, and hence improve the images. This was unsuccessful: Neither of the samples could be spread significantly, i.e., after both 0.1 and 10 s^{-1} , the yield stress of the samples with 20 vol. % particles was too high. This

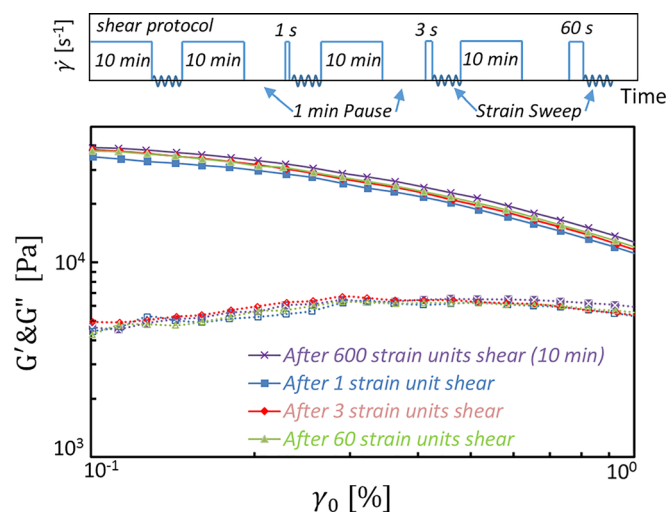


FIG. 6. LAOS results for ternary mixture (PIB/PEO/silica = 76.8/3.2/20) following the shear protocol sketched above. Filled symbols with solid lines represent the storage modulus and open symbols with dashed lines represent the loss modulus.

experiment was then repeated at a much lower particle loading of 3 vol. %, while maintaining the same PEO/PIB ratio ($\varrho = 0.16$). Here, the results proved clearer: The sample sheared at higher shear rate spread significantly, and discrete clusters can be readily identified by optical microscopy (Fig. 7). In contrast, the sample sheared at the lower rate did not spread significantly suggesting a larger yield stress, presumably due to larger interconnected clusters. Thus, we tentatively conclude that high rate shearing induces breakdown of capillary menisci, thus reducing the connectivity of the network. The shear thinning as noted in Fig. 3 (at fixed particle loading) or previously (at fixed ϱ) [12] may be attributed to this decrease in network connectivity. Confirming this tentative conclusion requires *in situ* visualization [43]. The present experimental system is ill-suited for *in situ* visualization: The large refractive index mismatch between the particles and the continuous phase makes it impossible to image samples with 20 vol. % particles. However, we conducted experiments on an analogous system comprising glass particles, 1,4-polyisoprene as the continuous phase, and glycerol as the wetting

fluid. Due to a near-perfect index match between the glass and polyisoprene, the particles are nearly invisible, and excellent images are obtained at 4.5 vol. % particles. Those experiments (Fig. S5 in the supplementary material [39]) show beyond doubt that meniscus-bound aggregates do break down at high rates, and moreover, they readily reform within a few strain units when sheared at low rate.

The third question above—how much strain pendular networks can withstand without undergoing irreversible deformation—was addressed by creep-recovery experiments. A sample of the same composition as in Fig. 2 (PIB/PEO/silica = 76.8/3.2/20) was subjected to creep at a stress of either 100 Pa or 150 Pa. Two stresses were needed to cover both “elastic” and “plastic” regimes of deformation (explained in the next paragraph), but note that both these stresses are lower than the yield stress measured in steady shear experiments [Fig. 4(a) and Table I] for this same sample. The creep was interrupted at a small strain, following which recovery was monitored. This was repeated at several different creep times. In between each creep step, the sample was “reset” by shearing at 1 s^{-1} for 600 strain units. These results are shown in Fig. 8(a).

The creep process (if not interrupted) comprises a rapid deformation to about 0.6% strain, followed by a slow increase in strain, as may be expected at a stress below the yield stress. Once interrupted, a portion of the strain recovered rapidly, followed by a slower recovery over several seconds. The ultimate recovery obtained from this experiment is shown in Fig. 8(b). If the applied strain is less than roughly 0.6%, almost all the strain can be recovered, i.e., the sample behaves elastically. Such elastic behavior is evident when the creep time is sufficiently small at 100 Pa strain. However, for larger strains, the ultimate recovery remains fixed, i.e., deformation in excess of $\sim 0.6\%$ is almost purely plastic. These correspond to the longer duration creeps at 100 Pa, and all the cases at 150 Pa stress. Similar results were obtained at other compositions, and two such examples ($\varrho = 0.04$ and $\varrho = 0.25$) are shown in Fig. S4 [39], respectively.

Plastic deformation is generally associated with irreversible microstructural changes. On the other hand, a glance at LAOS data such as Fig. 2 or 5(a) shows that the modulus at 0.6% oscillatory strain is already less than half of its value at small strain. This suggests that reversible strain softening occurs prior to plastic deformation. In order to verify this, one last experiment was conducted.

Samples were presheared at 1 s^{-1} for 10 min, and then subjected to oscillatory amplitude sweep tests where the upper limit of the amplitude was increased in each successive step. For instance, in Fig. 9, the first amplitude sweep ranged from 0.01% to 0.1% strain, the second from 0.01% to 1% strain, etc. It is clear that the modulus vs strain data remain reproducible at least up to 1% strain, a strain at which the modulus has reduced to less than half its low strain value. This confirms that significant modulus softening can occur reversibly, i.e., prior to irreversible decrease in modulus (see also [44] for further comments on this issue for a colloidal gel).

Figure 10 summarizes various strains that characterize the LAOS rheology: The limit of linearity ($\gamma_{critical}^*$) at which the G' reduces 10% from the value at the lowest strain accessible, the strain γ_{peak}^* at which the G'' shows a maximum, and the strain γ_{fluid}^* at which the G' and G'' cross. Two of these strain

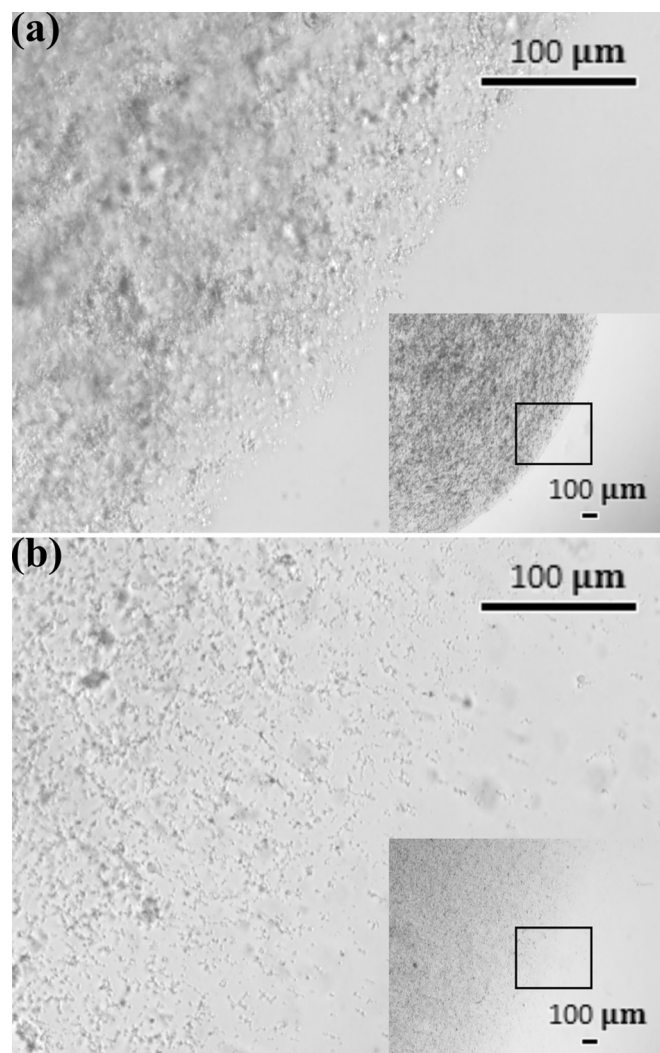


FIG. 7. Optical microscope showing ternary mixture (PIB/PEO/silica = 96.52/0.48/3) spreads on a petri dish: (a) after 0.1/s shearing for 10 min; (b) after 10/s shearing for 10 min. The insets show the same sample with lower magnification.

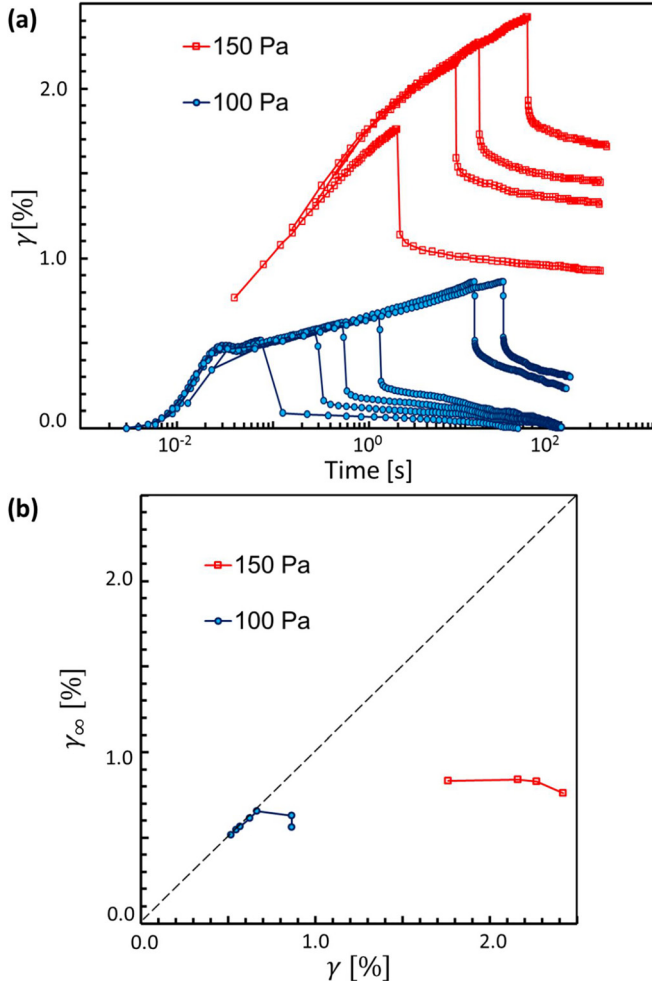


FIG. 8. (a) Creep-recovery test results for ternary mixture (PIB/PEO/silica = 76.8/3.2/20) at two stresses both below its yield stress. (b) Ultimate recovery strain (γ_∞) versus strain applied during creep (γ).

measures increase gradually with PEO content, whereas γ_{peak} decreases slightly. We note that γ_{fluid} disappears at low PEO content since there is no crossover ($G' < G''$ throughout the amplitude range). Furthermore, the sample with $\varrho = 0.004$ shows a weak peak in G'' and hence the corresponding value

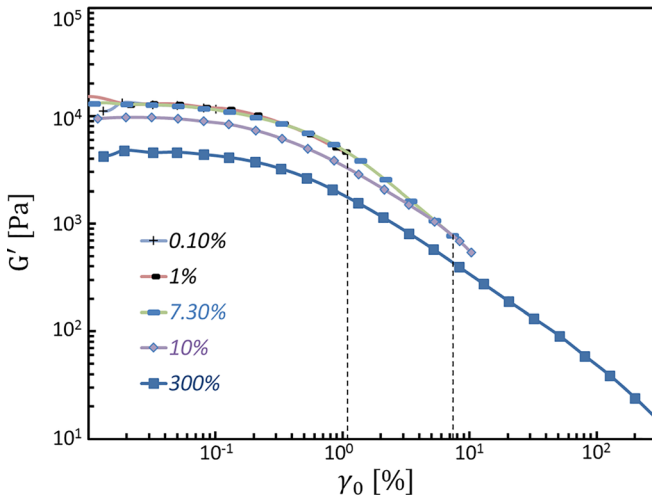


FIG. 9. LAOS results of ternary mixture (PIB/PEO/silica = 76.8/3.2/20) with sequentially increasing upper strain limit. Only storage modulus is shown.

of γ_{peak} is less reliable. At least one other article also mentions that the limit of linear viscoelasticity in LAOS experiments is only about 0.1%, although their crossover strains were larger [45]. Finally, above we also quantified two other measures of yielding: The strain at which irreversible changes in the linear viscoelastic modulus appear, and γ_∞ , the recoverable strain. Both these are on the order of 1%, and both increase slightly with wetting fluid content.

IV. DISCUSSION

Our microstructural picture of the suspensions in this study is of aggregates of particles held together by capillary forces, with the aggregates themselves percolating to form a network. In an ideal pendular network, all capillary interactions are strictly pairwise, i.e., each meniscus bridges exactly two particles, and there is no coalescence of menisci. The actual aggregates are not strictly pendular (indeed with poly-disperse systems, multiple particles sharing a meniscus is highly likely). Nevertheless, as a first approximation, we will consider the mechanics of pendular networks for the idealized case of pendular menisci, monodisperse particles, and monodisperse menisci. With these assumptions, a “volume balance” readily yields [11]

$$V_{meniscus} = \frac{8}{3z} \pi R_p^3 \frac{\phi_{PEO}}{\phi_p}, \quad (2)$$

where the value of z is the coordination number representing the average number of menisci per particle ($z = 4$ will be adopted below), and R_p is radius of the particles. One can therefore use Eq. (2) to estimate the mean meniscus volume from the composition of the ternary mixture. This meniscus induces an attractive force, F , between the particles. The meniscus force has a maximum magnitude of $2\pi R_p \alpha$ (where α is the interfacial tension) when the particles are in contact, $V_{meniscus}$ is small, and the meniscus fluid fully wets the particles. Thus, one may define a nondimensional force: $F^* = F/(2\pi R_p \alpha)$. Its dependence on interparticle separation is given by [30]

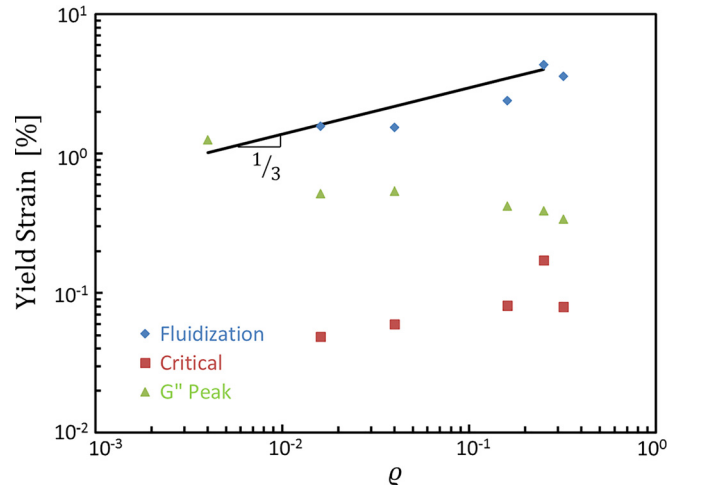


FIG. 10. Summary of various measures of yield strains: γ_{fluid} (blue diamond), $\gamma_{critical}$ (red square) and γ_{peak} (green triangle). Solid line with a slope of $1/3$ represents Eq. (5), but shifted down by a factor of 10.

$$F^* = \frac{\cos \theta}{1 + 2.1 \left(\frac{S^*}{\sqrt{V^*}} \right) + 10.0 \left(\frac{S^*}{\sqrt{V^*}} \right)^2} \text{ for } V^* < 10^{-5} \quad (3)$$

or

$$\ln F^* = f_1 - f_2 \exp \left(f_3 \ln \frac{S^*}{\sqrt{V^*}} + f_4 \left(\ln \frac{S^*}{\sqrt{V^*}} \right)^2 \right) \text{ for } 10^{-5} < V^* < 0.1, \quad (4)$$

where the f_j s are dimensionless variables which depend on V^* and liquid-solid contact angle θ [30]. For the sample compositions examined here, V^* exceeds 10^{-5} and hence only Eq. (4) is needed. In both these above expressions, $S^* = S/R_p$ is a nondimensional halfseparation (i.e., $2S$ is the separation between the particle surfaces), and $V^* = V_{meniscus}/R_p^3$ is a nondimensional meniscus volume [which can be estimated from Eq. (2)]. Note that F^* approaches 1 at small separations in Eq. (3). Beyond a certain separation, the meniscus ruptures, and the force jumps to zero. Previous results [46] show that the dimensionless half-separation for rupture is

$$S_c^* = \frac{1}{2} (V^*)^{\frac{1}{3}} = \frac{1}{2} \left(\frac{8}{3z} \pi \frac{\phi_{PEO}}{\phi_p} \right)^{\frac{1}{3}}, \quad (5)$$

where the latter equality is obtained from substituting from Eq. (2). The forces calculated from Eq. (4) [with Eq. (5) serving as the cut-off distance for meniscus rupture] are plotted in Fig. 11 for a variety of sample compositions. Several comments can be made based on this idealized model.

First, it is immediately tempting to ascribe rheological changes to breaking of the pendular menisci connecting the particles. For example, it is reasonable to expect that as the pendular network is sheared starting from quiescent conditions, irreversible changes appear when the particle separation exceeds that given by Eq. (5). This immediately suggests that if the deformation is affine, the breakdown strain should be roughly equal to S_c^* , and hence must scale as $\varrho^{\frac{1}{3}}$. Figure 10 shows that this scaling is approximately correct for all three measures of breakdown strain, although admittedly, the number of data points is small. We emphasize that this prediction presumes that z is independent of wetting fluid loading—an assumption that is guaranteed to break down at high ϱ values as menisci coalescence begins.

Second, the actual value of S_c^* predicted from Eq. (5) is far higher than estimated using any of the measures of breakdown. Specifically, the solid line in Fig. 10 is not a fit; it is Eq. (5) shifted down by a factor of 10. This overprediction remains regardless of what value of z is adopted, or even whether z is independent of ϱ or not (note that z is a coordination number and hence only values between 2 and 12 are physically realistic, and hence z cannot be too far from 4). This may indicate that breakdown of the network involves processes other than (or in addition to) meniscus breakdown. One candidate for other processes is simply the rearrangement of particles within the cages defined by their nearest neighbors. Indeed, past research on attractive suspensions

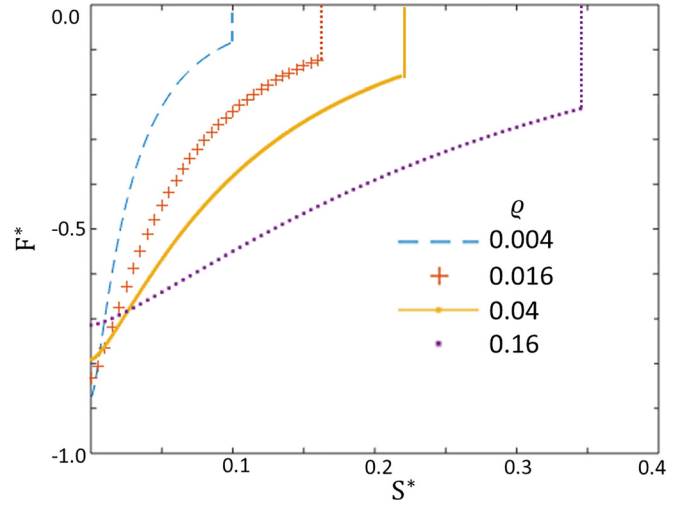


FIG. 11. Nondimensional capillary attractive force as a function of nondimensional half-separation distance between two particles for various ϱ values.

suggests that such particle rearrangement can induce permanent structural and rheological changes that are in addition to those attributable to interparticle attractions [47,48]. Another possibility is that breakdown may still involve meniscus rupture, but not homogeneously; instead, localized deformation may cause rupture of relatively few meniscus bonds which experience far higher strain than the average [49].

Third, a key experimental observation is the rate dependence of the modulus which we have attributed to structural breakdown (i.e. rupture of menisci) at high rates. It is useful to define a particle-scale capillary number

$$Ca_p = \frac{\text{viscous force}}{\text{interparticle adhesion}} = \frac{\eta \dot{\gamma} R_p^2}{2\pi R_p \alpha} = \frac{\eta \dot{\gamma} R_p}{2\pi \alpha}, \quad (6)$$

where η is the viscosity. The denominator is simply highest capillary force possible from Eq. (3). Thus, we expect that when Ca_p is on the order of 1, almost all interparticle capillary bonds are broken and the morphology consists of discrete particles wetted by the PEO, possibly coexisting with PEO drops that are no bigger than the particles. For $Ca_p \ll 1$ on the other hand, large meniscus-bound structures can survive. Previously [50], we have reported the interfacial tension, $\alpha = 0.082$ N/m, between PEO and PIB. The present polymers have somewhat different molecular weights, but in any case, α on the order of 0.01 N/m can be expected. Then with $R_p = 1 \mu\text{m}$ and $\eta = 10$ Pa s, we expect Ca_p to become on the order of 1 when $\dot{\gamma}$ is on the order of 6000 s^{-1} , a rate far exceeding the highest rate applied in our experiments. This simple dimensional analysis suggests that it is extremely unlikely that the shearing in our experiments is capable of breaking down the microstructure to the level of discrete particles. Thus, all the structural breakdown reported here is likely the rupture of menisci connecting multiparticle clusters, and small pendular clusters likely survive to the highest accessible rates.

Fourth, although we have previously drawn an analogy between such noncolloidal pendular suspensions and attractive colloidal suspensions [12], Fig. 11 illustrates some noteworthy

features specific to the pendular suspensions. For instance, in Fig. 11, the pairwise attraction extends to roughly 20% of the particle radius, whereas 5% of particle radius is more typical in attractive colloidal suspensions and gels (indeed some gels can be regarded as sticky hard spheres with negligible range of attraction [51–55]). Moreover, the pendular attraction is hysteretic: While an interparticle separation of $\sim 20\%$ of the particle diameter is needed to break the meniscus, the particles must be brought nearly into contact to restore the attraction. This may be one reason why a strain on the order of 1 induces modest breakdown of the sample (as judged by the slight modulus decrease in Fig. 6), which may be restored at higher strain. Indeed, at low particle loading, such hysteresis may become increasingly important: Reforming a meniscus requires the particles to collide with each other, and thus, we anticipate that once broken down after high-rate shearing, long shearing at lower rates may be needed to restore capillary menisci between particles. Finally, the interparticle repulsion, which corresponds to contact between the particle surfaces, is extremely short range. Thus, for all practical purposes, the force-displacement curve for the particles has a positive slope at all separations (i.e., greatest attractive force is at zero separation). This suggests that a chain of pendular menisci cannot deform homogeneously; instead, localized deformation and rupture of menisci is expected, analogous to pulling on a chain of magnets. Certainly, a three-dimensional network can deform in more complex ways than a single chain, but nevertheless, nonaffine deformation may appear even at low strains. In fact, we have conducted one preliminary experiment, albeit using the fluids and particles of Fig. S5 [39]. This experiment is described supplementary Fig. S6 [39] shows that even at 300% strain, there is little or no deformation evident on the scale of single particles. Instead, breakdown involves rotational motion of roughly rigid segments of the pendular network. Results from Bossler and Koos (personal communication) support localized rupture as well.

Finally, a key result of this paper is that the rheology depends on the shearing conditions prior to the measurements. This immediately points to the difficulty of quantifying rheological properties as a function of composition. For instance, in a previous article, we examined pendular suspensions along a specific path in the ternary composition diagram where wetting fluid was 16% of the particle loading. Along that path, we reported that the low-frequency plateau modulus as well as yield stress followed power laws, $G'_p \sim \phi_p^{4.9}$ and $\sigma_y \sim \phi_p^{3.3}$. In light of the results of this paper, if the shear history of the suspensions were changed, those power laws exponents may change or indeed the behavior may not remain power law at all.

V. SUMMARY AND CONCLUSIONS

In summary, this article makes two chief contributions. The first, an operational issue, is to develop a new method of preparing pendular networks. The key merit of this method is to mix the particles and the drops together under conditions under which the drops are frozen. Thus, the drop size distribution, contact angle, the stress under which drops collide with particles and wet them, etc., can all be kept consistent across a wide range of sample compositions. Obviously, this is only

possible when the drop fluid can be frozen by crystallization or vitrification. The second is to elucidate fundamentals of pendular network rheology. In this context, the chief observations of this article are (1) pendular networks undergo a significant loss of modulus upon shearing at high rates, likely due to rupture of pendular menisci joining the particles, (2) at least for the compositions examined, the changes in rheology can be reversed, i.e., sufficiently long shearing can reset flow-induced rheological changes, (3) pendular networks can show elastic recoil strains on the order of 1%, and yield at larger strains, and (4) they also undergo significant reversible decrease of modulus prior to yield.

Overall, the observations are consistent with the physical picture that a pendular network yields by rupture of the menisci joining particles. Nevertheless, the yield strains are far smaller than may be expected by simple considerations of how much two particles need to separate before the meniscus between them breaks. We speculate that this is because yielding and flow involve rupture of a relatively few menisci connecting large particle aggregates.

ACKNOWLEDGMENTS

The authors acknowledge the National Science Foundation for financial support (NSF-CBET Grant Nos. 0932901 and 1336311), Trystan Domenech (Fig. S1, supplementary material). The authors are grateful to Dr. Erin Koos, Karlsruhe Institute of Technology, for the use of her flow visualization apparatus and for assisting with the experiment of Figs. S5 and S6.

References

- [1] Halsey, T. C., and A. J. Levine, "How sandcastles fall," *Phys. Rev. Lett.* **80**, 3141–3144 (1998).
- [2] Herminghaus, S., "Dynamics of wet granular matter," *Adv. Phys.* **54**, 221–261 (2005).
- [3] Schanz, T., "Unsaturated soils: Experimental studies," in *Proceedings of the International Conference "From Experimental Evidence Towards Numerical Modeling of Unsaturated Soils,"* Weimar, Germany, September 18–19, 2003 (Springer, Berlin Heidelberg, 2006).
- [4] Andreotti, B., Y. Forterre, and O. Pouliquen, *Granular Media: Between Fluid and Solid* (Cambridge University, 2013), p. 161.
- [5] Vankao, S., L. E. Nielsen, and C. T. Hill, "Rheology of concentrated suspensions of spheres. 2. Suspensions agglomerated by an immiscible 2nd liquid," *J. Colloid Interface Sci.* **53**, 367–373 (1975).
- [6] Koos, E., and N. Willenbacher, "Capillary forces in suspension rheology," *Science* **331**, 897–900 (2011).
- [7] McCulfor, J., P. Himes, and M. R. Anklam, "The effects of capillary forces on the flow properties of glass particle suspensions in mineral oil," *AIChE J.* **57**, 2334–2340 (2011).
- [8] Lee, M. N., H. K. Chan, and A. Mohraz, "Characteristics of pickering emulsion gels formed by droplet bridging," *Langmuir* **28**, 3085–3091 (2012).
- [9] Dittmann, J., E. Koos, and N. Willenbacher, "Ceramic capillary suspensions: Novel processing route for macroporous ceramic materials," *J. Am. Ceram. Soc.* **96**, 391–397 (2013).
- [10] Domenech, T., and S. Velankar, "Capillary-driven percolating networks in ternary blends of immiscible polymers and silica particles," *Rheol. Acta* **53**, 593–605 (2014).

- [11] Heidlebaugh, S. J., T. Domenech, S. V. Iasella, and S. S. Velankar, "Aggregation and separation in ternary particle/oil/water systems with fully wettable particles," *Langmuir* **30**, 63–74 (2014).
- [12] Domenech, T., and S. S. Velankar, "On the rheology of pendular gels and morphological developments in paste-like ternary systems based on capillary attraction," *Soft Matter* **11**, 1500–1516 (2015).
- [13] Zhang, J., H. Zhao, W. F. Li, M. Xu, and H. F. Liu, "Multiple effects of the second fluid on suspension viscosity," *Sci. Rep.* **5**, 16058 (2015).
- [14] Domenech, T., J. Y. Yang, S. Heidlebaugh, and S. S. Velankar, "Three distinct open-pore morphologies from a single particle-filled polymer blend," *PCCP* **18**, 4310–4315 (2016).
- [15] Koos, E., "Capillary suspensions: Particle networks formed through the capillary force," *Curr. Opin. Colloid Interface Sci.* **19**, 575–584 (2014).
- [16] Haibach, K., A. Menner, R. Powell, and A. Bismarck, "Tailoring mechanical properties of highly porous polymer foams: Silica particle reinforced polymer foams via emulsion templating," *Polymer* **47**, 4513–4519 (2006).
- [17] Barbeta, A., G. Rizzitelli, R. Bedini, R. Pecci, and M. Dentini, "Porous gelatin hydrogels by gas-in-liquid foam templating," *Soft Matter* **6**, 1785–1792 (2010).
- [18] Lee, M. N., and Mohraz, A., "Bicontinuous macroporous materials from bijel templates," *Adv. Mater.* **22**, 4836–4841 (2010).
- [19] Ngai, T., S. A. F. Bon, H. J. Butt, I. Hamley, H. A. Stone, C. Wu, B. J. Park, P. Clegg, S. Biggs, and H. Zhao, *Particle-stabilized Emulsions and Colloids: Formation and Applications* (Royal Society of Chemistry, 2014), pp. 65–87.
- [20] Thareja, P., B. P. Ising, S. J. Kingston, and S. S. Velankar, "Polymer Foams stabilized by particles adsorbed at the air/polymer interface," *Macromol. Rapid Commun.* **29**, 1329–1334 (2008).
- [21] Dickinson, E., "Food emulsions and foams: Stabilization by particles," *Curr. Opin. Colloid Interface Sci.* **15**, 40–49 (2010).
- [22] Jin, H. J., W. Z. Zhou, J. Cao, S. D. Stoyanov, T. B. J. Blijdenstein, P. W. N. de Groot, L. N. Arnaudov, and E. G. Pelan, "Super stable foams stabilized by colloidal ethyl cellulose particles," *Soft Matter* **8**, 2194–2205 (2012).
- [23] Herzig, E. M., K. A. White, A. B. Schofield, W. C. K. Poon, and P. S. Clegg, "Bicontinuous emulsions stabilized solely by colloidal particles," *Nat. Mater.* **6**, 966–971 (2007).
- [24] Flemmer, C. L., "On the regime boundaries of moisture in granular materials," *Powder Technol.* **66**, 191–194 (1991).
- [25] Strauch, S., and S. Herminghaus, "Wet granular matter: A truly complex fluid," *Soft Matter* **8**, 8271–8280 (2012).
- [26] Aussillous, P., and D. Quere, "Liquid marbles," *Nature* **411**, 924–927 (2001).
- [27] Binks, B. P., and R. Murakami, "Phase inversion of particle-stabilized materials from foams to dry water," *Nat. Mater.* **5**, 865–869 (2006).
- [28] Duzyol, S., and A. Ozkan, "Correlation of flocculation and agglomeration of dolomite with its wettability," *Sep. Sci. Technol.* **46**, 876–881 (2011).
- [29] Velankar, S. S., "A non-equilibrium state diagram for liquid/fluid/particle mixtures," *Soft Matter* **11**, 8393–8403 (2015).
- [30] Willett, C. D., M. J. Adams, S. A. Johnson, and J. P. K. Seville, "Capillary bridges between two spherical bodies," *Langmuir* **16**, 9396–9405 (2000).
- [31] Butt, H. J., and M. Kappl, "Normal capillary forces," *Adv. Colloid Interface Sci.* **146**, 48–60 (2009).
- [32] Rallison, J. M., "The deformation of small viscous drops and bubbles in shear flows," *Annu. Rev. Fluid Mech.* **16**, 45–66 (1984).
- [33] Minale, M., J. Mewis, and P. Moldenaers, "Study of the morphological hysteresis in immiscible polymer blends," *AIChE J.* **44**, 943–950 (1998).
- [34] Burkhart, B. E., P. V. Gopalkrishnan, S. D. Hudson, A. M. Jamieson, M. A. Rother, and R. H. Davis, "Droplet growth by coalescence in binary fluid mixtures," *Phys. Rev. Lett.* **87**, 098304 (2001).
- [35] Oldroyd, J. G., "The elastic and viscous properties of emulsions and suspensions," *Proc. R. Soc. London Ser. A* **218**, 122–132 (1953).
- [36] Okamoto, K., M. Takahashi, H. Yamane, H. Kashihara, H. Watanabe, and T. Masuda, "Shape recovery of a dispersed droplet phase and stress relaxation after application of step shear strains in a polystyrene polycarbonate blend melt," *J. Rheol.* **43**, 951–965 (1999).
- [37] Vinckier, I., P. Moldenaers, and J. Mewis, "Elastic recovery of immiscible blends—I. Analysis after steady state shear flow," *Rheol. Acta* **38**, 65–72 (1999).
- [38] Nagarkar, S. P., and S. S. Velankar, "Morphology and rheology of ternary fluid-fluid-solid systems," *Soft Matter* **8**, 8464–8477 (2012).
- [39] See supplementary material at <http://dx.doi.org/10.1122/1.4973962> for results from additional rheological experiments, and images and a movie of the flow visualization experiments mentioned.
- [40] Coussot, P., "Rheological interpretation of velocity profiles," *Rheometry of Pastes, Suspensions, and Granular Materials* (John Wiley & Sons, Inc., 2005).
- [41] Coussot, P., "Structural similarity and transition from newtonian to non-Newtonian behavior for clay-water suspensions," *Phys. Rev. Lett.* **74**, 3971–3974 (1995).
- [42] Koos, E., and N. Willenbacher, "Particle configurations and gelation in capillary suspensions," *Soft Matter* **8**, 3988–3994 (2012).
- [43] Bossler, F., and E. Koos, "Structure of particle networks in capillary suspensions with wetting and nonwetting fluids," *Langmuir* **32**, 1489–1501 (2016).
- [44] Buscall, R., I. J. McGowan, P. D. A. Mills, R. F. Stewart, D. Sutton, L. R. White, and G. E. Yates, "The rheology of strongly-flocculated suspensions," *J. Non-Newtonian Fluid Mech.* **24**, 183–202 (1987).
- [45] Koos, E., W. Kannowade, and N. Willenbacher, "Restructuring and aging in a capillary suspension," *Rheol. Acta* **53**, 947–957 (2014).
- [46] Lian, G. P., C. Thornton, and M. J. Adams, "A theoretical study of the liquid bridge forces between 2 rigid spherical bodies," *J. Colloid Interface Sci.* **161**, 138–147 (1993).
- [47] Pham, K. N., G. Petekidis, D. Vlassopoulos, S. U. Egelhaaf, W. C. K. Poon, and P. N. Pusey, "Yielding behavior of repulsion- and attraction-dominated colloidal glasses," *J. Rheol.* **52**, 649–676 (2008).
- [48] Koumakis, N., and G. Petekidis, "Two step yielding in attractive colloids: Transition from gels to attractive glasses," *Soft Matter* **7**, 2456–2470 (2011).
- [49] Colombo, J., and E. Del Gado, "Stress localization, stiffening, and yielding in a model colloidal gel," *J. Rheol.* **58**, 1089–1116 (2014).
- [50] Thareja, P., and S. Velankar, "Rheology of immiscible blends with particle-induced drop clusters," *Rheol. Acta* **47**, 189–200 (2008).
- [51] Pantina, J. P., and E. M. Furst, "Directed assembly and rupture mechanics of colloidal aggregates," *Langmuir* **20**, 3940–3946 (2004).
- [52] Sedgwick, H., S. U. Egelhaaf, and W. C. K. Poon, "Clusters and gels in systems of sticky particles," *J. Phys.-Condens. Matter* **16**, S4913–S4922 (2004).
- [53] Dibble, C. J., M. Kogan, and M. J. Solomon, "Structure and dynamics of colloidal depletion gels: Coincidence of transitions and heterogeneity," *Phys. Rev. E* **74**, 041403 (2006).
- [54] Buzzaccaro, S., R. Rusconi, and R. Piazza, "'Sticky' hard spheres: Equation of state, phase diagram, and metastable gels," *Phys. Rev. Lett.* **99**, 098301 (2007).
- [55] Cardinaux F., A. Stradner, P. Schurtenberger, F. Sciortino, and E. Zaccarelli, "Modeling equilibrium clusters in lysozyme solutions," *EPL* **77**, 48004 (2007).